Biointerphases (2012) 7:59
DOI 10.1007/s13758-012-0059-1

ARTICLE

Changes in Permeability and in Mechanical Properties of Layer-by-Layer Films Made from Poly(allylamine) and Montmorillonite Postmodified upon Reaction with Dopamine

Vincent Ball · Kadir Apaydin · Abdelghani Laachachi · Valérie Toniazzo · David Ruch

Received: 17 July 2012 / Accepted: 27 August 2012 / Published online: 11 September 2012

Abstract Polyelectrolyte multilayer (PEM) films present a versatile surface functionalization method allowing to address many applications. These coatings suffer; however, from weak mechanical properties this problem can be addressed by the regular incorporation of clays in the layering process. To allow for an even better control of a whole set of film properties, among them their thermal stability, their stability in water, and their impermeability to anions, we postmodify $(PAH\text{-}MMT)_n$ films with polydopamine, by putting the pristine PEM films in contact with an oxygenated dopamine solution. This straightforward treatment allows to totally suppress the diffusion of hexacyanoferrate anions in the films and affects significantly its mechanical properties even, if the distribution of polydopamine through the film thickness is not yet known.

1 Introduction

Polyelectrolyte multilayer (PEM) films, obtained through the alternated adsorption of oppositely charged polymers [1] on either planar or colloidal supports [2], appear more and more an easy way to modify solid–liquid interfaces with coatings of controlled thickness, able to act as drug release systems and able to respond to an external stimulus like temperature [3], pH [4, 5], ionic strength [6], the presence of nanoparticles [7] and electromagnetic fields. The so called "layer-by-layer" deposition method yielding the PEM films can also be extended to polymers carrying hydrogen bond donors and acceptors [8, 9] as well as to inorganic colloids and polyelectrolytes [10]. The presence of hydrogen bond donor or acceptor moieties on the deposited random co-polyelectrolytes was shown to allow for molecular recognition [11] and hence showed the possibility to use PEM films as possible biosensors. Many examples of biosensing have been shown, since that time [12]. Even, if the deposition of PEM films or composite films made from polyelectrolytes and nanoparticles is easy and versatile, allowing to produce functional coatings for a wide range of applications [12–14], such films suffer mostly from weak adhesion to their substrate and from weak mechanical properties, notably a low resistance to wear [15].

Bioinspired composites mimicking the structure of nacre, made essentially of 95 % (in mass) of $CaCO_3$ and of 5 % of polymer binder, contain highly anisotropic particles separated by polymer binder, and are exceptionally robust materials displaying an intrinsic layered structure. [16] The first example of composite films made from the alternated adsorption of polycations and clays has been published in 1994 [17] and opened a wide research field allowing to produce extremely strong [18] and self standing membranes [19, 20]. An extensive review of all such kinds of composite films prepared through alternated adsorption of clays and polymers has been published recently [21]. Of major interest is to even reinforce such composite films made from clays and polymers to increase their toughness. One elegant method has been to use polycations modified

Electronic supplementary material The online version of this article (doi:10.1007/s13758-012-0059-1) contains supplementary material, which is available to authorized users.

V. Ball · K. Apaydin · A. Laachachi · V. Toniazzo · D. Ruch
Advanced Materials and Structures, Centre de Recherche Public Henri Tudor, 66 rue de Luxembourg, 4002 Esch-sur-Alzette, Luxembourg

V. Ball (✉)
Faculté de Chirurgie Dentaire, Université de Strasbourg, 1 Place de l'Hôpital, 67000 Strasbourg, France
e-mail: vincent.ball@tudor.lu; vball@unistra.fr

with catechol groups able to undergo an oxidative crosslinking reminiscent from the process occurring in *Mytilus edulis* foot proteins (*Mefp*) at the extremity of the byssus of mussels [22]. This crosslinking process allows for an extremely strong adhesion of the mussels to all kinds of substrates in conditions of extremely strong shear stresses. The oxidation of L-3,4-dihydrophenylanaline (L-DOPA), one of the major amino acids present with a high abundance in *Mefp* 3 and *Mefp* 5, inspired the use of catecholamines like dopamine to produce versatile coatings able to coat all kinds of substrates with a thin coating called polydopamine. Such a film shares many common properties with eumelanin, the major pigment of the skin and hair [23]. The synthesis of polydopamine in the presence of highly hydrated PEM films made from poly(-L-lysine) (PLL) and hyaluronic acid (HA) allowed to detach these films as free standing membranes, whereas the unmodified films underwent a complete decomposition during the detachment process. Even, if the mechanical properties of such membranes were not evaluated, it was shown that the mobility of the fluorescein labeled PLL chains (PLL-FITC) was significantly reduced with respect to the PLL-FITC chains in PEM films not put in contact with dopamine. [24] The presence of polydopamine in the PEM film is believed to create some chemical crosslinks owing to the reactivity of amine groups (from PLL) with the available catechols on polydopamine [25]. In order to reinforce multilayered films made from clays and polymers, Podsiadlo et al. [26] used L-DOPA modified polymers deposited in alternation with clays. An Fe^{3+} solution was then used to induce reticulation of the film in a postdeposition manner. This strategy allowed to obtain nanocomposite free standing films with an ultimate strength of about 200 MPa, whereas the films made from poly(diallyldimethyl ammonium chloride) and montmorillonite (MMT) displayed only 100 MPa.

In the present investigation we wish to use the strategy employed for the crosslinking of $(PLL\text{-}HA)_n$ films [22] to modify composite films made from the alternated deposition of poly(allylamine) (PAH) and MMT. We will give herein preliminary results showing that the optical properties, the permeability for a hexacyanoferrate anions and the elastic modulus of the $(PAH\text{-}MMT)_n$-polydopamine films are significantly modified with respect to that of the $(PAH\text{-}MMT)_n$ coatings. These films were deposited in conditions leading to an ultrafast growth of near 400 nm per deposition cycle, where one deposition cycle corresponds to the successive adsorption of the polycation and the clay [27]. Among the investigated properties, we will focus on the film's thickness, its refractive index (real and imaginary part), its permeability to redox probes like hexacyanoferrate anions, its thermal stability and its mechanical properties.

2 Experimental

2.1 Chemicals

Poly(allylamine chloride) (PAH) (Sigma-Aldrich, ref 28.322-3, Mw = 56,000 g mol^{-1}) was dissolved at 1 mg mL^{-1} in 50 mM Tris buffer which pH has been previously adjusted to 7.5 (±0.1) with hydrochloric acid (Across Chemicals). Dopamine hydrochloride (H 8502 from Sigma Aldrich) was dissolved at 2 g L^{-1} in the same Tris buffer just before the beginning of each experiment aimed to produce polydopamine in the composite $(PAH\text{-}MMT)_n$ films. Sodium montmorillonite (NaMMT) (from Southern Clay Co) was dissolved at 1 % (w/v) in water whose pH was previously adjusted to 10 (±0.1) with a diluted NaOH solution. This suspension was then sonicated for 1 h in an ultrasonic bath to ensure proper exfoliation of the clay. No sedimentation was observed even after days of storage in the absence of agitation. The clay platelets were adsorbed on glass slide covered with a PAH layer and imaged by means of Atomic Force Microscopy (AFM) in tapping mode, they display lateral dimensions of about 100–200 nm and an average thickness of 1 nm (data not shown). All solutions were prepared from doubly distilled water (Millipore Simplicity system, $\rho = 18.2$ MΩ cm). P doped silicon wafers (111 orientation) used as substrates for the deposition of the films, according to the LBL method were purchased from Siltronics, Archamps, France. These substrates were cleaned by immersion during half an hour in a 2 % v/v Hellmanex solution (Hellma GMbH), rinsed with distilled water, immersed a few minutes in a 0.1 M HCl solution, intensively rinsed with distilled water and blown dry with a stream of nitrogen.

2.2 Deposition of Polyelectrolyte Multilayer Films

The $(PAH\text{-}MMT)_n$ films were deposited by alternated dipping of the substrates (silicon wafer or PLA sheets) in solutions of PAH, buffer solution, clay suspension and water at pH 10. The buffer and water rinse steps were aimed to desorb weakly adsorbed PAH and clay, respectively. Each adsorption step lasted over 1 min. The samples were not blown dry between successive deposition steps, but dried after elaboration in an oven at 60 °C for 1 h as described our previous work [27].

2.3 Reaction of the $(PAH\text{-}MMT)_n$ Films with Dopamine

The substrates on which the $(PAH\text{-}MMT)_n$ films were deposited were hold vertically in a beaker glass to which a freshly prepared dopamine solution (2 g L^{-1} in the presence of Tris buffer at pH 7.5) was added. This solution was

slightly shaken during 14 h at 200 rotation min^{-1} with a magnetic stirrer. In the presence of oxygen, dopamine undergoes an oxidation/self assembly process yielding to polydopamine coatings on surfaces and the formation of particles in solution [23]. The silicon slides were then removed from the resulting polydopamine containing solution and intensively rinsed with distilled water before drying in an oven at 60 °C for 1 h.

2.4 Spectroscopic Ellipsometry

The thickness of the PEM films was calculated from spectroscopic ellipsometry measurements (Auto SE, Horiba, France) in the wavelength range between 450 and 1,000 nm and at a constant angle of incidence of 70°. The ellipsometric angles $\psi(\lambda)$ and $\Delta(\lambda)$ were used to calculate the film thickness and its refractive index using a three layer model in which the first layer was a semi infinite silicon substrate, the second layer a 2 nm thick SiO_2 layer spontaneously grown on silicon and the PEM film as the third layer, modeled as an homogeneous and isotropic layer. The dispersion law of indium tin oxide was used to fit the $n(\lambda)$ dispersion law of this third layer, made of the $(PAH\text{-}MMT)_n$ or $(PAH\text{-}MMT)_n$-@polydopamine films. The thickness and refractive index values given in the curves were the average (± one standard deviation) over three measurements performed along the major axis of the silicon wafer used to deposit the PEM films. For convenience, the refractive index values will be given at $\lambda = 632.8$ nm, corresponding to the wavelength of the He–Ne laser.

2.5 Electrochemical Measurements

All the electrochemical measurements, either cyclic voltammetry (CV) or impedance spectroscopy were performed with a Gamry 600 potentiostat in a three electrode configuration. The reference electrode was a KCl saturated Ag/AgCl electrode (CHi instruments, ref. 111) and the auxiliary electrode was a platinum wire (CHi instruments, ref. 115). The $(PAH\text{-}MMT)_n$ films were deposited on amorphous carbon working electrodes (CHi instruments ref. 104). The electrodes were polished with alumina paste for three cycles of polishing (each one lasting over 2 min) and then intensively sonicated in distilled water.

Before the deposition of the PEM film, CVs were acquired at 50 mV s^{-1} by cycling the potential difference between −0.10 and +0.70 V and back to −0.10 V versus Ag/AgCl at a scan rate of 50 mV s^{-1}. These CV curves were acquired in the presence of 10 mM Tris buffer + 150 mM NaCl with or without added potassium hexacyanoferrate at 1 mM (Sigma P9387). These experiments allowed for the determination of the capacitive current (in the absence of the redox probe) as well as to check the quality of the electrode polishing. The PEM film was deposited on the working electrode only if the potential difference between the potential corresponding to the maximum oxidation current and the potential of the maximum reduction current were not separated by more than 80 mV, the theoretical value being of 59 mV at 25 °C for a reversible one electron oxidation–reduction process.

After the deposition of the $(PAH\text{-}MMT)_n$ films, according to the previously defined protocol, the electrode was submitted to a series of potential scans in the presence of Tris-NaCl buffer, but in the absence of the redox probe in order to obtain the capacitive current curves. The electrode covered with the $(PAH\text{-}MMT)_n$ film was then put in contact with the same buffer containing 1 mM of potassium hexacyanoferrate. CV curves were measured after defined contact time between the electrode and the solution containing the redox probe. When the oxidation and reduction currents reached steady state values, corresponding to the sum of the capacitive and faradaic currents, we started an EIS experiment. In such a measurement, a constant bias of 0.25 V versus Ag/AgCl was applied, corresponding to a potential difference allowing for maximal oxidation current of hexacyanoferrate anions. To this DC signal we superimposed an alternating signal 5 mV in amplitude. The frequency of this AC potential difference varied between 10^5 and 10^{-2} Hz. 12 measurements were performed per frequency decade.

At the end of the acquisition of the EIS spectrum, we rinsed the electrode with Tris-NaCl buffer and measured the CV curves at regular time intervals and at a scan rate of 50 mV s^{-1} to follow the release of hexacyanoferrate anions from the film. The same experiments were performed for $(PAH\text{-}MMT)_{10}$-PAH film reacted with dopamine during 14 h. The films were put in contact with the hexacyanoferrate containing solution only after the deposition of polydopamine.

2.6 X-Ray Diffraction

X-ray diffraction (XRD) experiments were performed with an Inel France diffractometer. Samples were scanned in the reflection mode using the Cu Kα radiation ($\lambda = 1.5405$ Å, 45 kV, 40 mA).

2.7 UV–Vis and FTIR Spectroscopy

The MMT and PAH containing films were deposited on quartz slides (Thuet, Blodelsheim, France). These substrates were cleaned by immersion during half an hour in a 2 % v/v Hellmanex solution (Hellma GmbH), rinsed with distilled water, immersed a few minutes in a 0.1 M HCl solution, intensively rinsed with distilled water and blown

dry with a stream of nitrogen. PAH and MMT were deposited as indicated previously (1 min per adsorption step). The deposition was stopped after the deposition of *n* layer pairs and half of the films were used for modification with polydopamine as previously indicated. The absorption spectrum of the $(PAH\text{-}MMT)_n$ and of the $(PAH\text{-}MMT)_n$-@polydopamine coatings was measured with a double beam Lambda 35 spectrophotometer (Perkin Elmer) between 350 and 700 nm. An uncoated quartz slide was used as the reference in each case. The films were immersed in water for half an hour, dried in the oven during 1 h at 60 °C and their spectrum was measured again. Three hydration/drying cycles were performed to asses for the film stability in the presence of water.

The FTIR spectra of the film components and of the composite films were acquired on a Tensor 27 spectrometer (Bruker) with a resolution of 4 cm^{-1} in the transmission mode. To that aim, the films were scratched away from the deposition substrate and about 5 mg of the obtained powder was mixed with about 200 mg of dried KBr powder. 128 interferograms were accumulated to get a spectrum.

2.8 Scanning Electron Microscopy

Scanning Electron Microscopy (SEM) analyses were performed with an environmental microscope (FEI-Quanta 200 type). The distance between the sample and the detector used for x-ray measurement was 10 mm corresponding to a take-off angle of 35°. In the environmental SEM mode the samples were observed directly without the deposition of a conductive coating.

2.9 Thermogravimetric Analysis

The thermal degradation properties of freestanding $(PAH\text{-}MMT)_{10}$ films with and without polydopamine (14 h of reaction in the presence of a 2 g L^{-1} dopamine solution) were investigated by thermogravimetric analysis (TGA). The TGA apparatus was a NETZSCH-STA 409 PC, operating in air environment under a 100 cm^3 min^{-1} gas flow using alumina crucibles containing 10 mg of sample. The run was carried out, under air, in dynamic conditions with a gasflow of 100 cm^3 min^{-1} and at a constant heating rate of 10 °C min^{-1}.

2.10 Atomic Force Microscopy

The AFM topographies of the dried films were acquired in the tapping mode with a Dimension Fast Scan microscope (Bruker Nano Surfaces Division) at a frequency of 10 Hz and with a resolution of 512 × 512 pixels over a surface area of 1 × 1 μm. The used cantilevers were Fastscan-A (Bruker Probe) with 20 μm long V shape lever (f = 1.3 MHz, k = 15 N m^{-1}) and a silicone tip.

2.11 Mechanical Properties of the $(PAH\text{-}MMT)_n$ and of the $(PAH\text{-}MMT)_n$-@polydopamine Coatings

The $(PAH\text{-}MMT)_{10}$ and $(PAH\text{-}MMT)_{10}$-@polydopamine coatings were investigated by Peak Force Tapping mode with a colloidal probe (SQube, 1 μm diameter silica particle) using the Dimension Fast Scan. This mode allows collection of force curves at a rate of 2 kHz to map in parallel topography and mechanical properties. The obtained force curves were analyzed in real-time in the framework of the Derjaguin-Muller-Toporov (DMT) [28] model to obtain subsequent modulus mapping. Adhesion was also worked out as local minima along the force curve. The distribution of elastic moduli was plotted for the image with 512 × 512 pixels resolution. Typical time for mapping recording was less than 10 min. The spring constant of the colloidal lever was assessed by mean of thermal noise analysis, while the radius of curvature was confirmed by measuring the modulus of a reference polystyrene film.

3 Results and Discussion

The thickness of the $(PAH\text{-}MMT)_n$ films and of the same films put during 14 h in the presence of a dopamine solution (2 g L^{-1} in the presence of 50 mM Tris buffer at pH 7.5 and in the presence of magnetic stirring) was investigated by means of spectroscopic ellipsometry (Fig. 1). The film thickness hardly changed during the formation of polydopamine as well as the real part of the refractive index (plotted at a wavelength of 632.8 nm in Fig. 1) But the imaginary part of the film, reflecting the absorption of light, increased significantly after reaction with dopamine to yield polydopamine (Fig. 1c).

The increase in *k* traduces the appearance of new chromophores in the film. Such a result is expected, because polydopamine absorbs light over the whole UV–Vis spectrum in a manner similar to eumelanin [29]. Indeed the $(PAH\text{-}MMT)_{10}$ films turn black after 14 h of contact with an oxygenated dopamine solution (data not shown). The fact that the real part of the refractive index does not change during the formation of dopamine is not due to the non incorporation of polydopamine in the film (otherwise the film would not appear black after the reaction), but could be to the fact that the fraction of polydopamine incorporated is rather small or that the incorporation of the black pigment is accompanied by the release of some water and/or some counter ions present in the pristine $(PAH\text{-}MMT)_n$ films. These two assumptions are reasonable,

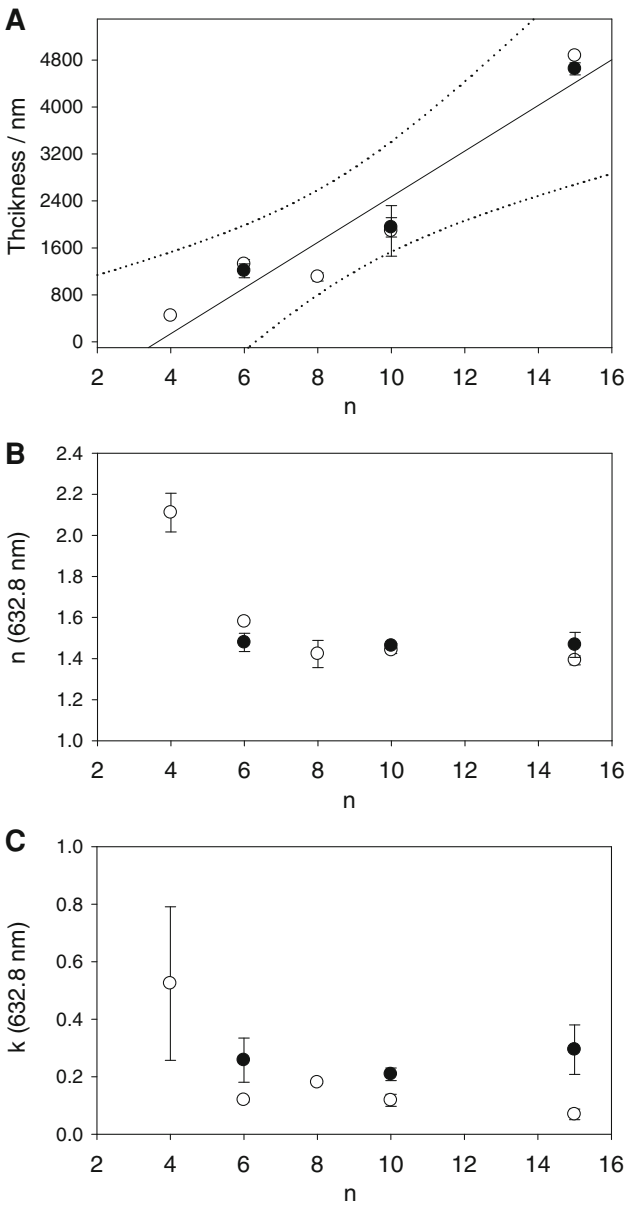

Fig. 1 Optical properties of $(PAH\text{-}MMT)_n$ films (*open circles*) as a function of the number of deposition cycles and of the same films after 14 h of contact with an aerated dopamine solution (*filled circles*, 2 g L^{-1} in the presence of 50 mM Tris buffer at pH 8.5). **a** Film thickness, the *full line* corresponds to a linear regression to the experimental data (slope 389 nm per layer pair) and the *dotted lines* to the limit of the 95 % confidence interval. **b** Real part of the refractive index at $\lambda = 632.8$ nm. **c** Imaginary part of the refractive index at $\lambda = 632.8$ nm. The *error bars* correspond to one standard deviation over three measurements on the same sample. All the films where prepared in an independent experiment

because polydopamine has a real part of the refractive equal to 1.73 at 632.8 nm [30] much higher than that of the $(PAH\text{-}MMT)_n$ films ($\sim$1.45 for $n > 4$; Fig. 1b). Note also that the film growth rate was extremely high, about 390 nm per deposition cycle, as in our previous report where the $(PAH\text{-}MMT)_n$ films were deposited in identical conditions [27]. This result is highly unexpected on the basis of the expected thickness for a monolayer of clay combined with a monolayer of PAH, namely a few nanometers. Podsiadlo et al. [31] already reported the occurrence of exponential film growth in which MMT was deposited every fourth layer. These films displayed a very high thickness increment per deposition cycle even, if it was expected that the introduction of MMT should strongly hinder the diffusion of polyelectrolytes in and out of the films. We observe, in the present study, that the films made from more than $n = 6$ adsorption cycles have a gel like appearance and that they are strongly deformed, when dried under a nitrogen stream. Such a finding was also reported by Podsiadlo et al. [31]. For that reason, the films were hold horizontally and dried in an oven at 60 °C for 1 h before characterization by means of spectroscopic ellipsometry. Complementary to these findings, the reaction with dopamine during 14 h and the subsequent drying of the film at 60 °C during 1 h seems not to alter the ordered arrangement of the clay sheets in the direction parallel to the plane of the film as observed in SEM cross-sections (Fig. 2). The cross sections of the films modified by polydopamine look similar to those of unmodified $(PAH\text{-}MMT)_n$ films prepared in the same conditions (Fig. 1 of the supplementary material). However, the films put in the presence of dopamine seem to have much more defects. In addition, the XRD results show us, on the one hand a peak at $2\theta = 7.2°$ with a d_{hkl} of 12.3 Å corresponding to the neat MMT and on the other hand two peaks shifted at 5.96° ($d_{hkl} = 14.75$ Å) and 6.10° ($d_{hkl} = 14.33$ Å) for $(PAH\text{-}MMT)_{10}$ coatings having undergone or not 14 h of reaction with an aerated dopamine solution (Fig. 3). According this results, we assume that the interaction between MMT and PAH is somewhat modified when the films are reacted with dopamine. The width of the diffraction peaks diminishes in the $(PAH\text{-}MMT)_{15}$ and $(PAH\text{-}MMT)_{15}$-@polydopamine films with respect to the peaks of pure MMT probably in reason of the alignment of the clay particles in the direction parallel to the substrate during the layering process, as shown in the SEM micrograph of Fig. 2. Our observations are consistent with the findings of Jaber and Lambert [32] who reported the formation of a composite when L-DOPA is reacted in the presence of Laponite. It appeared that the presence of the clay considerably accelerated the formation of the melanin like material and that the composition of this material was different from that obtained in the absence of Laponite, decarboxylation of the indole rings occurred during the formation of the nanocomposite material [32].

In addition, we do not yet know the distribution of polydopamine through the thickness of the film, and if the chosen reaction time was sufficient to reach the steady state of the chemical reaction leading to polydopamine. We aim to investigate this point by means of confocal Raman

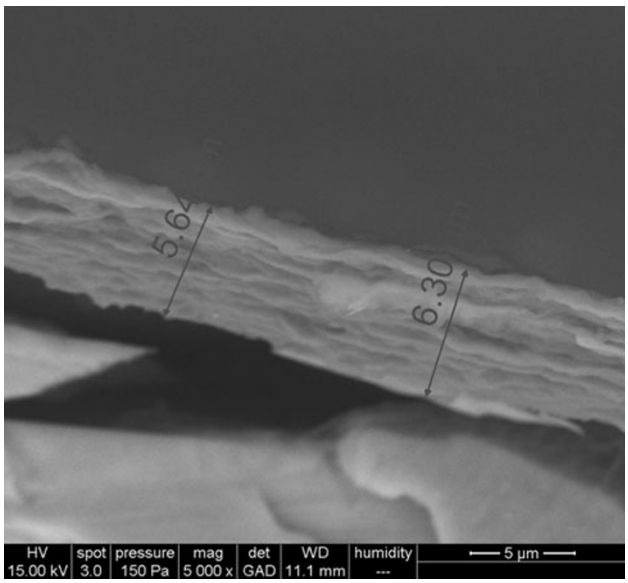

Fig. 2 SEM cross sectional image of a $(PAH\text{-}MMT)_{15}$ film reacted during 14 h with a dopamine solution (2 g L^{-1} in the presence of 50 mM Tris buffer at pH 8.5)

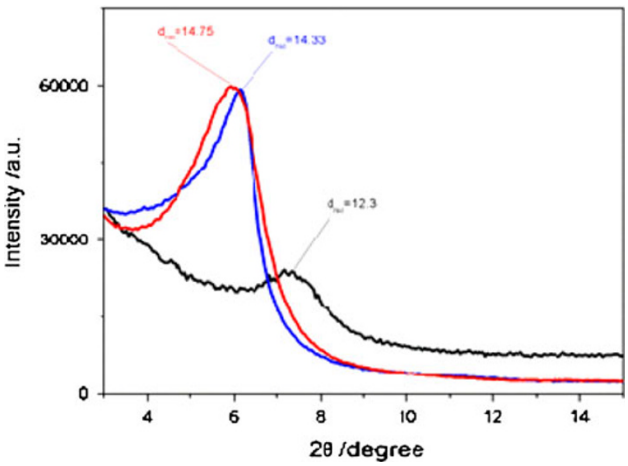

Fig. 3 Diffractogramm of the MMT powder (*black line*), of the $(PAH\text{-}MMT)_{15}$ film before (*blue line*) and after (*red line*) 14 h of reaction with a 2 g L^{-1} dopamine solution in the presence of 50 mM Tris buffer at pH 7.5. The d_{hkl} values are given in Angströms

microscopy, because eumelanin displays a Raman spectrum close to that of disordered graphite [33]. Confocal Raman spectroscopy will also allow for some accurate depth profiling with a resolution close to 1 µm. To that aim we need; however, to use much thicker coatings as those characterized in the present work.

The absorbance increase at 500 nm of a $(PAH\text{-}MMT)_{10}$@-polydopamine film with respect to a $(PAH\text{-}MMT)_{10}$ reference film is however, much larger (0.16 units) than the absorbance increase of a naked quartz slide put during 14 h in an oxygenated dopamine solution (0.04 units). This suggests that the polydopamine deposited in the $(PAH\text{-}MMT)_{10}$ film is much important than the ~35 nm thick layer grown on quartz in these conditions [34]. Even if the reaction time of 14 h between the film and the oxygenated dopamine solution may not be sufficient to fill the film homogenously with polydopamine through its whole thickness, it was nevertheless sufficient to significantly modify the properties of the $(PAH\text{-}MMT)_n$ films, as will be shown below. The FTIR spectra of $(PAH\text{-}MMT)_{10}$ films as well as those of its individual constituents are shown in Fig. 3 of the supporting material. The spectrum of the $(PAH\text{-}MMT)_{10}$ film after reaction with a dopamine solution during 14 h is hardly different from the spectrum of the pristine film most probably, because the FTIR spectrum of polydopamine display broad peaks between 1,700 and 1,100 cm^{-1} [24] which are very close to the peaks already present in the unmodified film. However, the change in the films colour, becoming black after formation of polydopamine, as well as the change in their thermal degradation (see below) shows that polydopamine is present in the film.

The TGA curves (Fig. 4) show that polydopamine synthesized in solution undergoes three main degradation steps: one at around 120 °C most probably associated with the desorption of strongly bound water, one between 260 and 330 °C and the last one at 545 °C. The unmodified $(PAH\text{-}MMT)_{10}$ films display two peaks in their DTG curve at 257 ± 2 and at 617 ± 2 °C. The ATG and DTG curves of the $(PAH\text{-}MMT)_{10}$-@polydopamine films exhibit a much more complex behaviour; the peaks near 260 and 600 °C are close to that of the unmodified film, whereas two new peaks at 496 and 877 °C, not observed for polydopamine prepared in solution, are found. The $(PAH\text{-}MMT)_{10}$-@polydopamine films have a residual mass of 40 ± 1 %, whereas the unmodified $(PAH\text{-}MMT)_{10}$ films leave 56 ± 1 % of their mass, the lost mass being mainly due to water release and decomposition of PAH. These results imply that $(PAH\text{-}MMT)_{10}$-@polydopamine contains about 15 weight% of polydopamine, which has nevertheless a different behavior (and perhaps a different composition and structure) than the polydopamine prepared in the MMT free Tris buffer. The polydopamine obtained in the $(PAH\text{-}MMT)_n$ films may be quite different in composition and in structure than the polydopamine produced in solution. This difference may be due to the presence of the clay, as suggested by Jaber and Lambert [32], but also due to the presence of PAH which can interact with the catechol group of polydopamine via its primary amino groups [25].

The polydopamine modified coatings were extremely stable in water in marked contrast with the unmodified $(PAH\text{-}MMT)_n$ films (Fig. 2 of the supplementary material) successive immersions in water followed by drying did not change the absorption spectrum of the films, whereas the unmodified films underwent at least 70 % decrease in

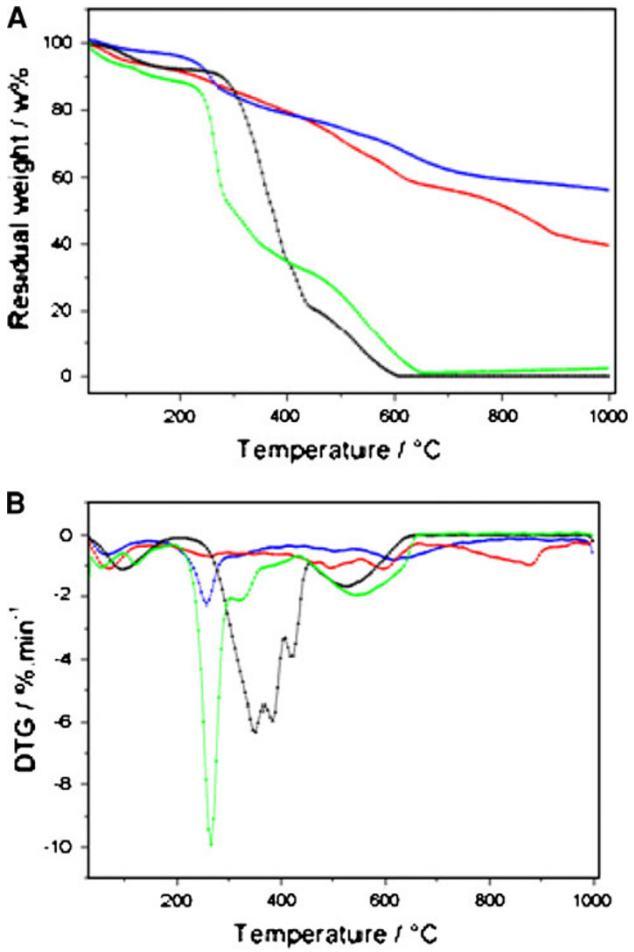

Fig. 4 TGA (**a**) and DTG curves (**b**) of PAH (*black line*), polydopamine produced in solution (*green line*), $(PAH\text{-}MMT)_{10}$ (*blue line*) films and of $(PAH\text{-}MMT)_{10}$-@polydopamine (*red line*) films

absorbance after three drying-rehydration cycles. This resistance to water rinsing steps is crucial for future real life applications of such composite films.

The electrochemical properties of the $(PAH\text{-}MMT)_{10}$-@polydopamine coatings were also markedly different from those of the corresponding unmodified films which interact strongly with hexacyanoferrate anions and are able to retain them even after rinse with the Tris-NaCl (at 150 mM) buffer [27]. After reaction with dopamine during 14 h, the films became totally impermeable to the used redox probe (Fig. 5).

This finding shows that the incorporation of polydopamine to the $(PAH\text{-}MMT)_n$ films provides them with barrier properties with respect to anions, the unmodified films displaying already excellent oxygen barrier properties [27]. Nevertheless, herein we did not investigate, if the addition of polydopamine in the composite coatings did improve its barrier properties for oxygen. This will be the subject of a future work. It might well be possible that the presence of many polydopamine clusters and the associated defects

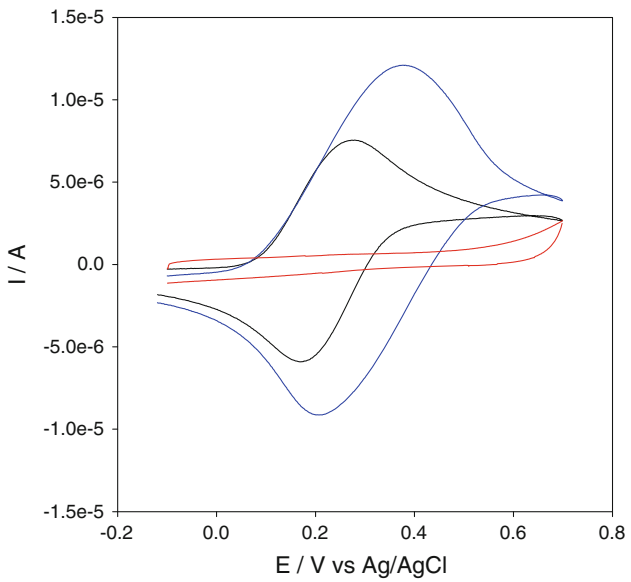

Fig. 5 Cyclic voltammetry experiments performed on the amorphous carbon electrode (*black line*) on the electrode modified with a $(PAH\text{-}MMT)_{10}$-PAH film (*blue line*) and on the same film after 14 h of reaction with dopamine (*red line*), the reaction being performed with dopamine at 2 g L^{-1} in the presence of 50 mM Tris buffer at pH 7.5. The redox probe was $K_4Fe(CN)_6$ at 1 mM in the presence of Tris 50 mM + NaCl 150 mM at pH 7.5

(Fig. 2) may considerably decrease the oxygen barrier properties of the $(PAH\text{-}MMT)_n$-@polydopamine coatings with respect to those of the unmodified films. Good barrier properties against hexacyanoferrate anions are not unexpected based on the observation that polydopamine coatings deposited on glassy carbon electrodes are highly impermeable to these anions. [35] In addition, polydopamine binds strongly to PAH via its amino groups [25] and induces probably a significant reduction of the permeability of the whole composite film. Complementary to the CV experiments, electrochemical impedance spectroscopy confirmed that the total impedance of the $(PAH\text{-}MMT)_{10}$ coating increased markedly after 14 h of reaction with an oxygenated dopamine solution (Fig. 4 of the supplementary material). However after only 2 h of reaction with an aerated dopamine solution, the permeability for hexacyanoferrate anions of the composite film is almost not affected with respect to the pristine film.

The morphology of the $(PAH\text{-}MMT)_{10}$ and of the $(PAH\text{-}MMT)_{10}$-@polydopamine films was investigated by means of AFM in the non contact mode, the root mean squared roughness of the coatings was found to be of 35.7 and 31 nm, respectively for these coatings showing that the deposition of polydopamine in the film and/or on its surface induces almost no change in the film morphology. (Fig. 5 of the supplementary material). Complementary, the mechanical properties of the pristine and polydopamine modified films were investigated by means of colloidal

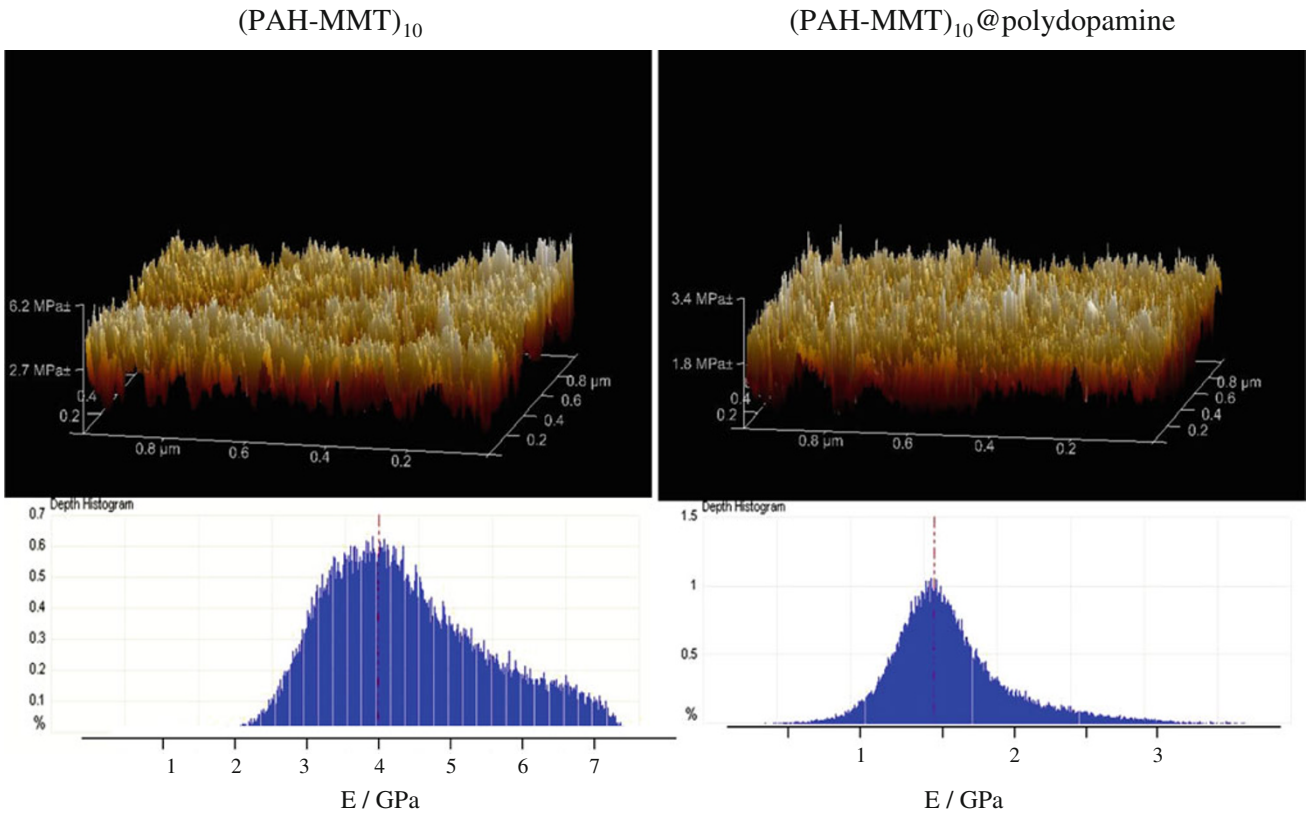

Fig. 6 Distribution of the elastic modulus (512 × 512 pixels) over 1 × 1 µm surfaces of $(PAH\text{-}MMT)_{10}$ and $(PAH\text{-}MMT)_{10}$-@polydopamine films

probe AFM. It appears that the average elastic modulus of the $(PAH\text{-}MMT)_{10}$-@polydopamine films, 1.5 ± 0.3 GPa, is two times lower than that of the pristine $(PAH\text{-}MMT)_{10}$ coating, where the distribution of moduli is bimodal, with a first peak at 4.5 ± 1.0 GPa and a second one at 7.0 ± 1.0 GPa (Fig. 6). The fact that the elasticity of the film somewhat decreases after reaction with dopamine to produce polydopamine is somewhat deceiving, but it is accompanied by an homogenization of the values of the local elastic moduli (Fig. 6).

Our results are different from those of Podsiadlo et al. [26] who showed that LBL films containing polycations modified with L-DOPA groups, become more rigid after the reticulation of the L-DOPA groups in the presence of Fe^{3+} cations. In the present case, where the $(PAH\text{-}MMT)_n$ films were modified with polydopamine after the deposition of the PEM film, it might well be that polydopamine which allows to establish crosslinks between amino groups carried by the polycation, induces a decrease of the strength of the interactions between the polycation and the clay. Another possible or complementary explanation for a slight decrease in the films elasticity is an overall increase in the fraction of organic material in the composite film as revealed by TGA (Fig. 4). The addition of polydopamine in the composite film may add some defects contributing to the decrease in the film's modulus. Even if the average elastic modulus decreases after reaction with dopamine to form polydopamine, the PEM films become impermeable to redox probes like hexacyanoferrate (Fig. 5) and also display a better adhesion with the colloidal probe used to perform the AFM experiments. Namely, over 1 × 1 µm surface areas, the adhesion force between the $(PAH\text{-}MMT)_{10}$-@polydopamine film and the silica probe glued on the cantilever was of 49 ± 3 nN, whereas it was only of 38 ± 2 nN for the $(PAH\text{-}MMT)_{10}$ film. This finding is not unexpected owing to the well known behaviour of polydopamine films to be mimics of *Mefp* proteins in mussels [36]. In addition, whereas the $(PAH\text{-}MMT)_{60}$ films can be detached from the deposition substrate as a free standing membrane by a single peeling process [27], it seems that the adhesion of the polydopamine modified films with the glass substrate is significantly improved impeding its easy detachment. This finding opens the route for the fabrication of robust multilayer films with improved adhesion to their deposition substrate which is a prerequisite for many industrial applications.

4 Conclusions

In the present investigation, we showed preliminary data showing the possibility to modify the optical, electrochemical

and mechanical properties of multilayered films made from PAH and MMT when such films are exposed for prolonged time (here 14 h) to a dopamine solution in the presence of oxygen as an oxidant. In these conditions, polydopamine is produced in the solution. After modification with polydopamine, the films undergo up to 15 % increase in their organic content, but the thermal decompositions steps in the temperature range above 500 °C are different than for polydopamine produced in solution. This might well be due to a different oxidation and self-assembly pathway in the presence of the clay, as already demonstrated by Jaber and Lambert [32]. This assumption is also supported by the finding that the formation of polydopamine in the composite film is accompanied by some additional exfoliation of the clay. At the present stage of our investigation we do not yet know if polydopamine fills the film homogeneously through their section, but the amount of available black pigment is sufficient to drastically modify the permeability of the coating for hexacyanoferrate anions and to reduce somewhat the elastic modulus of the films. This decrease in stiffness is however compensated by an homogenization of the values of the local elastic moduli and by an increase in the adhesive properties of the whole coating. In the future, we aim at investigating the wear resistance and the friction coefficient of such composite films containing polycations, clays and polydopamine.

Acknowledgments Kadir Apaydin is supported by an AFR grant from the FNR (Luxembourg). Dr. Samuel Lesko (Bruker) is acknowledged for having performed the AFM colloidal probe measurements.

References

1. Decher G (1997) Science 277:1232–1237
2. Donath E, Sukhorukov GB, Caruso F, Davies SA, Mohwald H (1998) Angew Chem Int Ed 37:2202–2205
3. Liao T, Moussallem MD, Kim J, Schlenoff JB, Ma T (2010) Biotechnol Prog 26:1705–1710
4. Zhai L, Cebeci FÇ, Cohen RE, Rubner MF (2004) Nano Lett 4:1349–1353
5. Tong W, Gao C, Möhwald H (2006) Macromolecules 39:335–340
6. Mjahed H, Voegel J-C, Senger B, Chassepot A, Rameau A, Ball V, Schaaf P, Boulmedais F (2009) Soft Matter 5:2269–2276
7. Srivastava S, Ball V, Podsiadlo P, Lee J, Ho P, Kotov NA (2008) J Am Chem Soc 130:3748–3749
8. Sukhishvili S, Granick S (2000) J Am Chem Soc 122:9550–9551
9. Laschewsky A, Wischerhoff E, Denzinger S, Ringsdorf H, Delcorte A, Bertrand P (1997) Chem Eur J 3:34–38
10. Kotov NA, Dékány I, Fendler H (1995) J Phys Chem 99:13065–13069
11. Caseli L, Dos Santos DS, Foschini M, Gonçalves D, Oliveira ON (2006) J Colloid Interface Sci 303:326–331
12. Srivastava S, Kotov NA (2009) Acc Chem Res 41:1831–1841
13. He Q, Cui Y, Li J (2009) Chem Soc Rev 38:2292–2303
14. Gao L, Fei J, Zhao J, Cui W, Cui Y, Li J (2012) Chem Eur J 18:3185–3192
15. Pavoor PV, Gearing BP, Bellare A, Cohen RE (2004) Wear 256:1196–1207
16. Aksay IA (1996) Science 273:892–898
17. Kleinfeld ER, Ferguson GS (1994) Science 265:370–373
18. Fan XW, Park MK, Xia CJ, Advincula R (2002) J Mater Res 17:1622–1633
19. Tang Z, Kotov NA, Magonov S, Ozturk B (2003) Nat Mater 2:413–418
20. Podsiadlo P, Kaushik A, Arruda EM, Waas AM, Shim BS, Xu JD, Nandivada H, Pumplin BG, Lahann J, Ramamoorthy A, Kotov NA (2007) Science 318:80–83
21. Podsiadlo P, Shim BS, Kotov NA (2009) Coord Chem Rev 253:2835–2851
22. Sever MJ, Weisser JT, Monahan J, Srinivasan S, Wilker JJ (2004) Angew Chem Int Ed 43:448–450
23. Lee H, Dellatore SM, Miller WM, Messersmith PB (2007) Science 318:426–430
24. Bernsmann F, Richert L, Senger B, Lavalle P, Voegel J-C, Schaaf P, Ball V (2008) Soft Matter 4:1621–1624
25. Lee H, Rho J, Messersmith PB (2009) Adv Mater 21:431–434
26. Podsiadlo P, Liu Z, Paterson D, Messersmith PB, Kotov NA (2007) Adv Mater 19:949–955
27. Laachachi A, Ball V, Apaydin K, Toniazzo V, Ruch D (2011) Langmuir 27:13879–13887
28. Derjaguin BV, Muller VM, Toporov YP (1975) J Colloid Interface Sci 53:314–326
29. Meredith P, Powell BJ, Riesz J, Nighswander-Rempel SP, Pederson MR, Moore EG (2006) Soft Matter 2:37–44
30. Bernsmann F, Ponche A, Ringwald C, Hemmerlé J, Raya J, Bechinger B, Voegel J-C, Schaaf P, Ball V (2009) J Phys Chem C 113:8234–8242
31. Podsiadlo P, Michel M, Lee J, Verploegen E, Wong Shi Kam N, Ball V, Lee J, Qi Y, Hart AJ, Hammond PT, Kotov NA (2008) Nano Lett 8:1762–1770
32. Jaber M, Lambert J-F (2010) J Phys Chem Lett 1:85–88
33. Huang Z, Lui H, Chen XK, Alajlan A, McLean DI, Zeng H (2004) J Biomed Opt 9(6):1198–1205
34. Bernsmann F, Ball V, Adieggo F, Ponche A, Michel M, Gracio JJ, Toniazzo V, Ruch D (2011) Langmuir 27:2819–2825
35. Bernsmann F, Voegel J-C, Ball V (2011) Electrochim Acta 56:3914–3919
36. Lee BP, Messersmith PB, Israelachvili JN, Waite JH (2011) Ann Rev Mater Res 41:99–132